Article

Real-Time Management for an EV Hybrid Storage System Based on Fuzzy Control

Dimitrios Rimpas *[ID], Stavros D. Kaminaris, Dimitrios D. Piromalis [ID] and George Vokas [ID]

Department of Electrical & Electronics Engineering, University of West Attica, 250 Thivon Av.,
122-44 Egaleo, Greece; skamin@uniwa.gr (S.D.K.); piromali@uniwa.gr (D.D.P.); gvokas@uniwa.gr (G.V.)
* Correspondence: drimpas@uniwa.gr; Tel.: +30-210-5381581

Abstract: Following the European Climate Law of 2021 and the climate neutrality goal for zero-emission transportation by 2050, electric vehicles continue to gain market share, reaching 2.5 million vehicles in Q1 of 2023. Electric vehicles utilize an electric motor for propulsion powered by lithium batteries, which suffer from high temperatures caused by peak operation conditions and rapid charging, so hybridization with supercapacitors is implemented. In this paper, a fuzzy logic controller is employed based on a rule-based scheme and the Mamdani model to control the power distribution of the hybrid system, driven by the state of charge and duty cycle parameters. An active topology with one bi-directional DC-to-DC converter at each source is exploited in the MATLAB/Simulink environment, and five power states like acceleration and coasting are identified. Results show that the ideal duty cycle is within 0.40–0.50 as a universal value for all power states, which may vary depending on the available state of charge. Total efficiency is enhanced by 6%, sizing is increased by 22%, leading to a more compact layout, and battery life is extended by 20%. Future work includes testing with larger energy sources and the application of this management strategy in real-time operations.

Keywords: battery; ultracapacitor; hybrid; energy; management; fuzzy; control

MSC: 93C42

1. Introduction

The need for a cleaner environment and the reduction of greenhouse gases has been identified as the primary target for the global population. The Paris Agreement of 2015 and the European Climate Law of 2021 set the need for a reduction of mean global temperature by two degrees Celsius via green transportation adoption by 2050 [1]. With those regulations, a 55% reduction in greenhouse gases is expected to be achieved. This margin is mainly focused on the road transport sector and especially light-duty passenger cars powered by internal combustion engines (ICE), which represented over 25% of total carbon dioxide emissions over the last five years, and are expected to increase until 2030 [2]. Therefore, decarbonizing the transportation sector and increasing energy efficiency in all other sectors is imminent for the protection of the environment [3].

Over the last 20 years, the trend of green transportation and improving fuel efficiency has led to hybrid (HEV) and battery electric vehicles (BEV). HEVs utilize an electric motor to assist the ICE or even power the car fully in conditions like traffic or low-speed driving. Hence, fuel consumption can be limited up to 30% in certain conditions without any significant changes in driving habits [4]. Due to their manufacturing simplicity, low emissions, and public demand for a sustainable price, a market share of 28% for EVs was achieved in 2021. However, the road to emission-free transportation can only be fully accomplished with the adoption of pure electric vehicles (EVs). An electric motor is responsible for the propulsion of the vehicle powered by lithium batteries and an advanced battery management system [5]. There are major benefits to the utilization of EVs like:

- No greenhouse gases emissions;
- Noiseless operation;
- Energy recovery through regenerative braking;
- Ability to charge at home via renewable sources.

These parameters played a major role in the recent sales of EVs. Up to 12% of the market share for 2022 is pure electric, with huge waiting lists due to the limited resources that manufacturers face, with diesel cars declining [6]. This trend is expected to continue strongly in 2023, with almost 2.5 million EVs sold in the first quarter, about to reach 15 million units in total, resulting in 35% year-on-year escalation and 18% of the total market share. By following this direction, 5 million crude oil barrels can be saved per day by 2030, ensuring the utilization of green environmental transportation means. Additional policies and measures are shown in Figure 1.
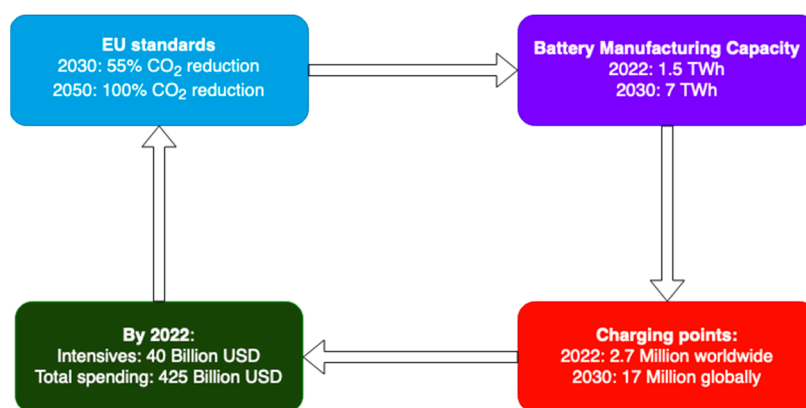

Figure 1. Policies and actions required for full electrification of the light duty vehicles [6].

However, there are still certain limitations regarding the operation of EVs, as summarized in previous work [5]. High charging time, a lack of chargers, low mileage causing range anxiety, and increased purchase costs as rare minerals are required for current battery and motor manufacturing are still considered major and practical limitations. It is evident that the main issues refer to the battery pack's limited operational conditions and sensitivity to extreme setups. The temperature window of a typical lithium battery is within 20 to 65 degrees Celsius, while functioning outside this range can cause lithium deposition, dendrites, or even total breakdown [7]. Proper cooling is crucial for protecting the cells from overheating, and while unified with the climate control system, it can decrease total energy consumed while offering maximum thermal comfort [8]. Additionally, charging and discharging sequences are supervised and controlled by complex power electronics to ensure safety and protection, avoiding peak conditions. As the battery is a part of the vehicle chassis for better weight management, even maintenance is practically unfeasible, so the layout has to be precisely designed and sized.

There are certain parameters affecting battery life [9–13]. State of charge (Soc) and state of health (SoH), which reveal the degradation of the cells, are crucial to calculating battery aging and cannot be measured directly on the pack. State of Power (SoP) supplies information about the battery's peak current capabilities, while state of voltage refers to the ratio of current-voltage divided by the nominal value and can be connected to the SoC. Lastly, Depth of Discharge (DoD) represents the percentage that the battery pack is discharged and proved to be valuable as a low DoD massively affects battery degradation, limiting stress on the cells and increasing its viability. It is essential to monitor all values to ensure battery-safe operation and nominal performance within the projected time applied by the manufacturer, as depicted in Figure 2.
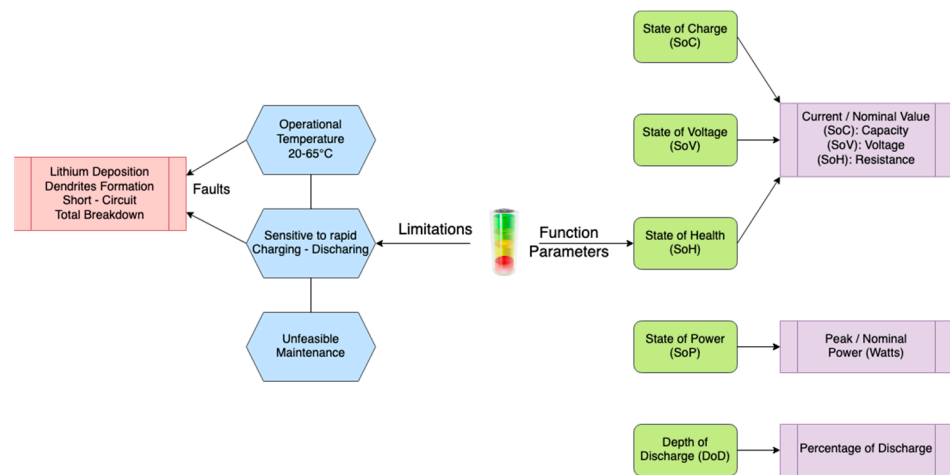
Figure 2. Limitations and operational parameters for a lithium battery.

To address those restrictions, a hybrid energy storage system (HESS), consisting of batteries and supercapacitors, is utilized. In everyday use, battery life is shortened due to significant heat generation caused by the need to cover the high power requirements of electrically powered vehicles [14]. Supercapacitors (SC) or ultracapacitors (UC) solve this problem by providing both average and peak power loads, reducing the maximum current of the battery by up to 55% and ensuring lower voltage drops, hence fewer fluctuations and capacity costs [15,16]. SC also inherits a lifespan of over 1 million operating cycles, making it the perfect auxiliary source. However, since the energy density is low, they cannot operate as a standalone source for an EV.

The combination of these different systems enables electric vehicles to operate over a longer range using high-energy-density batteries while increasing performance with ultracapacitors acting as power buffer units. In addition, the supercapacitor takes advantage of regenerative braking harvesting, providing better control and up to 16.2% more range with less wear [17]. The system performs greatly in low-temperature conditions where conventional batteries are outside their safety zone. However, the connection of power modes, as well as the duty cycle indication are not studied widely in the literature. The power demand has to be classified into different states for better understanding, and the operation cycle or duty cycle, namely the energy used in each time interval compared to the maximum, e.g., acceleration, are important parameters of proper power distribution.

The purpose of this work Is the implementation of a fuzzy logic simulation model for the operation of HESS via MATLAB/Simulink. This model calculates the various parameters affecting the hybrid system states (SOC, SOH, etc.) to manage the power split between the two sources connected in active topology. The introduction of duty cycle and power mode sequences is also a major step in designing the ideal scheme for power distribution, which is the contribution of this paper. Additionally, the energy management strategy (EMS) will be validated for enhanced efficiency of the system with constant protection of the battery cells.

The manuscript is structured into five main sections. Section 2 describes the equations and the methodology used to conduct the experiment, along with an explanation of duty cycles term and classification of the distinct power modes. In Section 3, the results of the simulation are presented. In Section 4, discussion about the outcome and comparison with other works is thoroughly examined. In the last section, conclusions about the model are included along with suggestions about future work.

2. Materials and Methods

2.1. Methodology

2.1.1. Hybrid Storage System Bank

The topology of the applied HESS is a key parameter in the power-split and dynamic performance of the whole setup. There are three different topologies: Passive, semi-active, and active [5]. In passive configuration, the two sources are simply connected in parallel, reducing peak currents adequately, but the ultracapacitor voltage is limited by the battery bank [18]. Semi-active format, which requires a DC-to-DC converter plugged into the battery or the SC while the other is connected in parallel with the converter, offers better cell protection and HESS sizing, but the layout is restricted by a low performance-to-cost ratio and increased converter sizing. Lastly, active topology implies two bi-directional converters directly connected to both the energy sources (battery and SC) and then toward the DC bus powering the motor and other electronics. Both sources can be coupled or decoupled from the load simultaneously. This arrangement was chosen for this project as performance, control, efficiency, and voltage regulation are the main priorities, even though it is by far the most complex setup. Power distribution is vastly configurable, offering the ability to test different energy management strategies [19]. The projected topology is depicted in Figure 3 below.
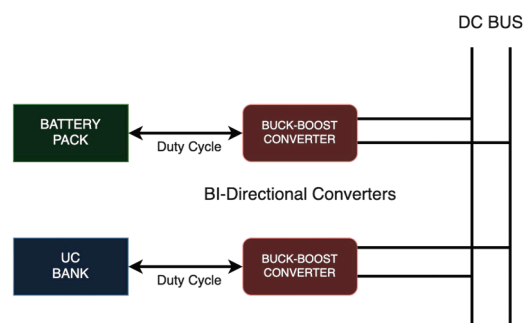

Figure 3. Experimental layout with two buck-boost converters connected directly to the DC bus with power output directly connected to power mode and duty cycle.

For calculations, the power loss model is considered. Since the internal parameters of both converters cannot be neglected, like inductor resistance, voltage drop, and switch on-resistance, the assumption that both models are identical, as found in [20], will be utilized. The power loss of the DC/DC components is related to the term known as the duty cycle. This describes the percentage that each source operates until it is recharged again, for example, 80% to 30% SoC and off to recharging, which complies with 50% duty cycle. As it is suggested, the duty cycle is expressed as the energy supplied by each source to cover the projected power demand within specified time interval. A 30% drop in the ultracapacitor SoC required to cover the vehicle acceleration from stop is also indicated as 30% duty cycle. It is renowned that small duty cycles and low charging times or rates (total amperage drawn), are essential for prolonging battery lifetime or prevent any possible breakdown as well as increasing charging capacity [21]. To calculate the power loss, the following equations are required [20]:

$$\text{Boost mode}: \begin{cases} P_{VEHICLE} - V_H \times I_{UC} = V_L \times I_B - P_{CON,LOSS} \\ \frac{P_{VEHICLE}}{V_H} = I_{UC} + I_B \times (1 - D_{BOOST}) \end{cases} \tag{1}$$

$$\text{Buck mode}: \begin{cases} P_{VEHICLE} - V_H \times I_{UC} = V_L \times I_B + P_{CON,LOSS} \\ \frac{P_{VEHICLE}}{V_H} = I_{UC} + I_B \times D_{BUCK} \end{cases} \tag{2}$$

where P_D is the power demand of the vehicle, $P_{CON,LOSS}$ refers to the power loss of the converter, V_H equals to voltage of the low voltage side, V_L is the high voltage value,

I_B is the DC/DC inductor current, mainly affecting the battery, I_{UC} denotes the current of the supercapacitor, and D_{BOOST} and D_{BUCK} represent the duty cycles at boost and buck modes, respectively.

Accordingly, further processing with the conversation of power and Kirchhoff's current law shows that the power loss of the total system is equal to the square of the inductor's current multiplied by internal resistances, the duty cycles at each state, and the voltages of the switches of the converters, which cannot be neglected [20]:

$$P_{CON,LOSS} = \begin{cases} I_B \times [\,(V_S + V_D) \times D_{BOOST}\,] + \times I_B^2 \times [R_L + (R_S + R_D) \times D_{BOOST}] \\ I_B \times [\,(V_S + V_D) \times D_{BUCK}\,] + \times I_B^2 \times [R_L + (R_S + R_D) \times D_{BUCK}] \end{cases} \tag{3}$$

where V_D and R_D are the voltage drop and resistance of the diode, V_S and R_S denote the voltage drop and resistance of the switch, and R_L refer to the inductor resistance [20].

2.1.2. Energy Sources Models

As every component and energy source, battery and supercapacitor can be simplified following Thevenin modeling for better explanation, ignoring losses that are infinitesimal. So, the battery model consists of the internal resistance R_B, the polarization voltage V_P, polarization capacitance C_P, polarization resistance R_P, and Terminal voltage V_T. V_{OC} accounts as the open circuit voltage, thus the maximum voltage the battery can provide with no load. So, the final model is presented in Figure 4 below [20].
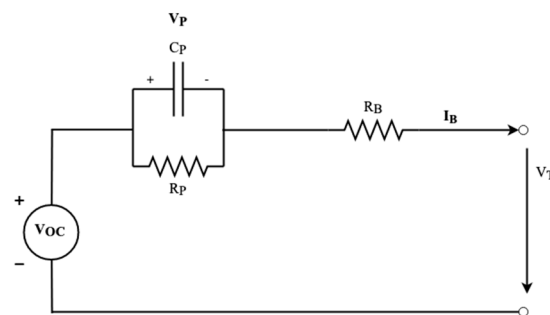

Figure 4. Lithium Battery Thevenin model by [20].

Depending on the state of charge and temperature at each specific time k, the polarization values are different and the terminal voltage has to be calculated from equations by [20,21]. It is obvious that these parameters are always in a dynamic state and must be supervised by the energy management system for further adjustments, improving efficiency and control.

$$V_{T(k)} = V_{OC} \times SOC_{(k)} - I_{B(k)} \times R_B \times SOC_{(k)} - V_{P(k)} \tag{4}$$

State of charge, at the time k is expressed at the next equation.

$$SOC(k) = \left(\frac{V_{P(k)} + V_{T(k)}}{V_{OC}} \right) \tag{5}$$

Finally, the lithium battery losses $P_{B,LOSS}$ can be calculated at any specific time k including all losses induced by polarization and internal resistance [20].

$$P_{B,LOSS} = I_B^2 \times R_B \times SOC + \frac{V_P}{R_P \times SOC} \tag{6}$$

The ultracapacitor can be simplified as an RC model or a electrical model containing the equivalent series resistance (ESR) or heat losses, the equivalent parallel resistance (EPR), representing leakage current and capacitance [22]. However, this model adds complexity to the simulation, so the RC model is preferred. For simplicity, both rated capacitance

(C_R) and internal resistance (R_{UC}) will be accounted consistently even though they differ during charging-discharging due to the effects of ESR and EPR. V_{UC} and I_{UC} represent the ultracapacitor voltage and current, with V_T as the voltage terminal, similar to the battery layout. Figure 5 illustrates the final model of the supercapacitor.
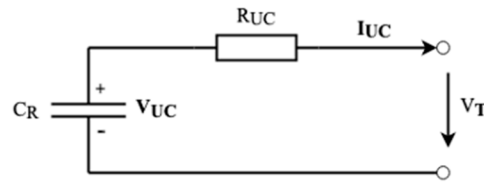

Figure 5. Supercapacitor RC model [20–22].

Since the model has been simplified, it is now possible to calculate all values, along with the power losses, by utilizing Kirchhoff's laws. The next Equations (7)–(11) modified from [20–22] are expressing these computations.

The Open circuit voltage of the ultracapacitor at a certain n time:

$$V_{UC(n)} = VUC(n-1) - \frac{I_{UC(n)}}{C_R} \tag{7}$$

Next is the equation for the terminal voltage of the SC at n time:

$$V_{T(n)} = V_{T(n-1)} - I_{UC(n)} \times R_{UC} \tag{8}$$

The total power delivered by the ultracapacitor is expressed as:

$$P_{UC(n)} = V_{T(n)} \times I_{UC(n)} \tag{9}$$

The current flowing in and out of the capacitor is calculated with Equation (10). The same equation applies for charging or discharging with a minus when the capacitor is being charged:

$$I_{UC} = \frac{V_{UC} - \sqrt{V_{UC}^2 - 4 \times R_{UC} \times P_{UC}}}{2 \times R_{UC}} \tag{10}$$

Equation (11) shows the power losses due to internal resistance and leakage current:

$$P_{UC,LOSS} = R_{UC} \times I_{UC}^2 \tag{11}$$

The state of voltage, similar to SOC for supercapacitors equals to the terminal voltage divided by the maximum rated voltage by the manufacturer as presented in Equation (12) [23].

$$SOV = \frac{V_T}{V_{RATED}} \tag{12}$$

Equation (13) is applied to calculate the state of health parameter revealing battery lifetime where charge is expressed as capacity, measured in ampere-hours [12].

$$\mathbf{SOH} = \frac{Qmax}{Qrated} \tag{13}$$

Finally, the total power losses of HESS plus the converter are calculated with Equation (13) below [14,20].

$$P_{LOSS,TOTAL} = P_{CON,LOSS} + P_{B,LOSS} + P_{UC,LOSS} \tag{14}$$

2.1.3. Duty Cycles

As mentioned previously, the duty cycle is an essential term for proper energy management and power distribution. The SOC, SOV, and other parameters should be maintained

high to cover the necessary power for the electric motor. At fractional levels, battery overcharging or discharging will lead to the end of the service life or even a failure. It is crucial to keep the frequency fixed without major fluctuations while keeping the state of charge of both sources above 25% as a lower threshold for protection and efficiency [22–24]. The topology chosen offers great control through buck-boost mode by the converters, along with fast power switching for adjustments in different power modes, minimizing voltage ripple and losses. Since the efficiency of the DC/DC can reach over 94% at average power/current outputs, the duty cycle should be low and focused on maintaining the SC charge high, thus keeping the converter at its rated power area [23–25].

The hybrid energy system Is required to cover the driving power demand $P_{VEHICLE}$ of the vehicle which is described in Equation (15) below [23].

$$P_{VEHICLE} = \frac{V_A}{3600 * \eta} \times (M \times g \times f \times \cos(\beta) + M \times g \times \sin(\beta) + \frac{C_{ARC} \times A}{21.15} * V_A{}^2 + \frac{\delta \times M}{3.6} \times \frac{dV_A}{dt}) \quad (15)$$

where V_A is the car speed, η denotes the powertrain efficiency, M is the total mass, g is the gravitational acceleration, f and C_{ARC} represent the rolling assistance and air resistance coefficients, β indicates the road incline, A is the wind exposed area and δ designates the rotation mass coefficient correction factor.

Based on Equation (14), the size of HESS utilized must be able to meet and overcome the power demand of the vehicle. For safety reasons, the battery power alone should also be able to meet this requirement, so the total number of cells, needed capacitance, and voltage are expressed at Equation (16) [23].

$$U_R \times C_R \times n_P \times n_S \geq P_{VEHICLE} \quad (16)$$

where U_R is the rated voltage, C_R denotes the rated capacitance of each cell, n_P indicates the battery cells required in parallel and n_S represents the cells in series.

2.1.4. Power Modes

There are various power modes for an EV based on the motor, and HESS states [24–26]: Initialization: When the vehicle starts, HESS needs to provide high torque quickly. At this time, the power is only provided by the SC, taking advantage of its high-power density. During acceleration, high current is required, so the battery should assist the SC in covering the motor power demand. The battery voltage is stepped up by a DC-DC converter to obtain a high DC bus voltage; hence, the HESS provides the energy required. The output power ratio of these sources should be reasonably distributed, with the supercapacitor providing most of the power and minimizing losses. However, as the voltage of SC decreases, the duty cycle lessens, so power losses can be minimized by discharging the lithium-ion battery and the ultracapacitor simultaneously. As a result, HESS can perfectly adapt to future instantaneous power demand.

The next mode is regenerative braking. If the vehicle is decelerating or coasting at high speeds, the engine is running as a generator and is in a power-generating state. The electrical energy generated is sent back to the HESS, almost entirely on the SC, to avoid high-frequency current on the battery. Then, depending on the state of charge of each source, energy is strategically distributed. During the braking phase, the voltage of the DC busbar is low and the DC/DC duty cycle is small. When the voltage of the ultracapacitor is higher, the DC/DC duty cycle is smaller, so losses are minimal.

Finally, in coasting, or cruising mode, the motor is running at constant speed due to a low load or road slope; thus, only a small current may be required. Therefore, SC is used to supply all load currents, as it is sufficient. The battery DC-DC converter is temporarily switched off to reduce circuit losses. However, if the SC voltage drops below the battery voltage, the battery can supply energy to the drive and charge the SC.

2.2. Fuzzy Model

For this project, the deployment of a fuzzy logic model via MATLAB/Simulink is selected. Fuzzy logic is a math model leading to a non-binary state of mind and a sophisticated control system [27]. Fuzzy control systems consist of four main parts: fuzzification, rule-based, fuzzy reasoning, and defuzzification. The power requirement is a valuable operating parameter and a key factor in the project. Even though increased processing power is required to run the models, there are multiple benefits regarding the use of FL strategy and controllers [28,29]. They are as follows:

1. Voltage regulation of the DC bus during load variations;
2. Limited battery current and frequency fluctuations hence lower temperatures;
3. High performance, simplicity, reliability, and enhanced lifetime;
4. The linearity pattern of data acquisition is a crucial parameter for a fuzzy model. A weighted memory H controller is utilized at [30] for increased precision in non-linear monitoring and identification of memory states based on Takagi-Sugeno fuzzy systems. The Wavelet packet decomposition method can be utilized for time sequence determination for consistent data retrieval, identification of charging or discharging states, and even power mode classification [31]. In addition, fuzzy logic modeling can be applied not only to EVs but also to smaller applications like electric scooters or three wheelers as well, limiting fluctuations and enhancing range [32].
5. The developed fuzzy set-based controller has five inputs: Power demand, UC, and battery voltages, and SoC. The controller uses a list of fuzzy rules to manipulate the correlation between inputs and outputs. According to the principles, efficient energy management must be provided with respect to the operating conditions of the energy source [33]. The supply is based on the SoC of each source and the power modes described before, which may also indicate the driving style [34]. The basic relationship between input and output, as defined by the fuzzy rules, is that the battery acts as the main energy source for the vehicle as long as the SOC is above 25% and the voltage of the ultracapacitor is below 50%.
6. At constant speeds with low energy consumption, energy is provided by the lithium battery, while the SC should be saved for peak demand loads like high slopes and rapid accelerations. Additionally, supercapacitors are efficient in regenerative braking exploitation since their high power density allows swift charging, even with high-frequency currents. Afterwards, SC can charge the battery or utilize a low-pass filter for that case to avoid high frequencies. The rules that comprise the fuzzy model are the following [35,36]:
7. Power demand and SOC_{SC} are M to H:SC will provide the demand entirely.
8. Power demand is H and SOC_{SC} is ML: SC will provide its available power.
9. Power demand is M to H and SOC_{SC} is L: Both sources output will be balanced.
10. Power demand is L to ML and SOC_{SC} is L: Again, sources are balanced.
11. Power demand is ML and SOC_{SC} is L: Battery will cover the power mostly.
12. Power demand is L to ML and SOC_{SC} is M to H: SC will provide most of the power.

Where L is low, ML stands for Medium Low, M for Medium and H for High. The scale is represented as a percentage as follows:

13. Low: 0–25%
14. Medium Low: 25–50%
15. Medium: 50–75%
16. High: >75%

The fuzzy control aims to generate commands for charging and discharging the two energy sources as a function of the fuzzy logic controller, presented in Table 1.

Table 1. Rules for the proposed fuzzy logic controller.

Power State	Power Output	
	SC	Battery
Regenerative braking	Charging *	Charging *
Coasting	Charging	Charging
Initialization	Maximum	Low
Slow Acceleration	Medium	Medium
Fast Acceleration	High	Medium

* Depending on SoC and duty cycle.

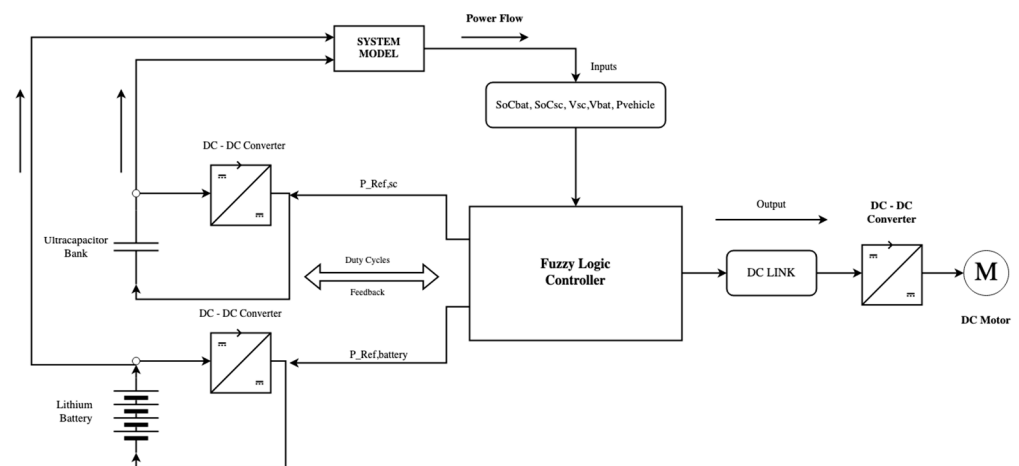The scheme selected for the EV is presented at Figure 6 below.

Figure 6. Experimental layout highlighting the power flow to the motor through the converter and the importance of the fuzzy logic controller.

Next, the power management flowchart shows the strategy followed by the FL controller to cover the power demand and handle the output of both sources. Membership functions are shown in previous works [32–38], based on the Mamdani model, and are projected in this paper as illustrated in Figure 7. The fuzzy model incorporates a small difference in rule definition (low to high) to specify the value of temperature and duty cycle in the power distribution scenarios implemented.
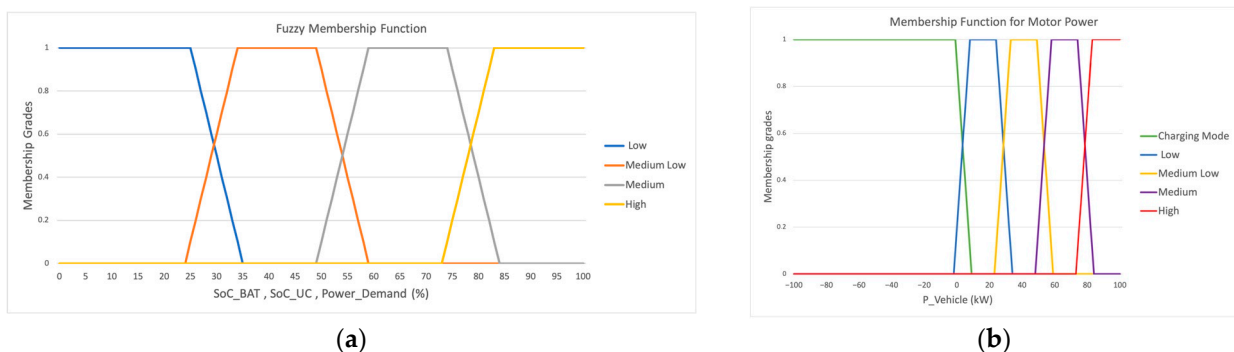

(**a**)

(**b**)

Figure 7. Membership functions utilized for this fuzzy model (**a**) Distinct energy sources SoC to cover the power demand; (**b**) Motor power ($P_{VEHICLE}$ parameter) function depending on the power state.

The regulation of charging and discharging as well as energy demand coverage are priorities shown in Figure 8 below:
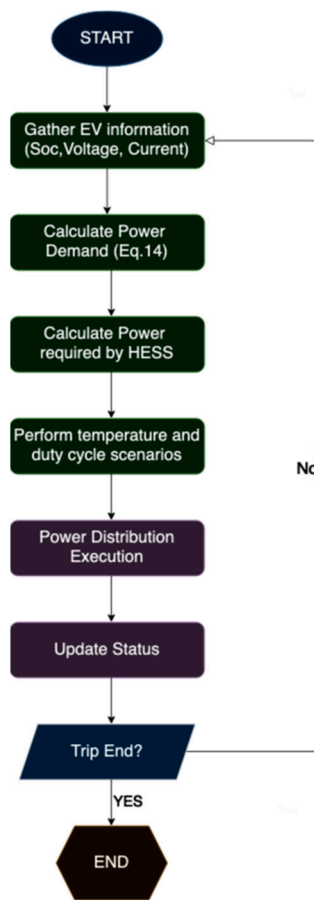
Figure 8. Fuzzy logic controller scheme as utilized in this work.

The power distribution ratios will vary depending on the state of charge of each source, as previously mentioned. In previous work, a specific ratio of 70% battery and 30% supercapacitor was presented to offer better sizing, cost, and weight, but with a modestly lower range [39]. Over 100,000 values validated the result, while temperature management and prevention of high-frequency currents provided increased battery life. This dataset will be utilized in this study, as well as a more advanced and precise control pattern is followed. However, control and charging were conducted manually at [39] so the limitations were escalated. The modelling of the fuzzy logic controller is implemented through MATLAB/Simulink via the ready-to-use libraries. Therefore, the diagram of this model in the application environment is projected in Figure 9.
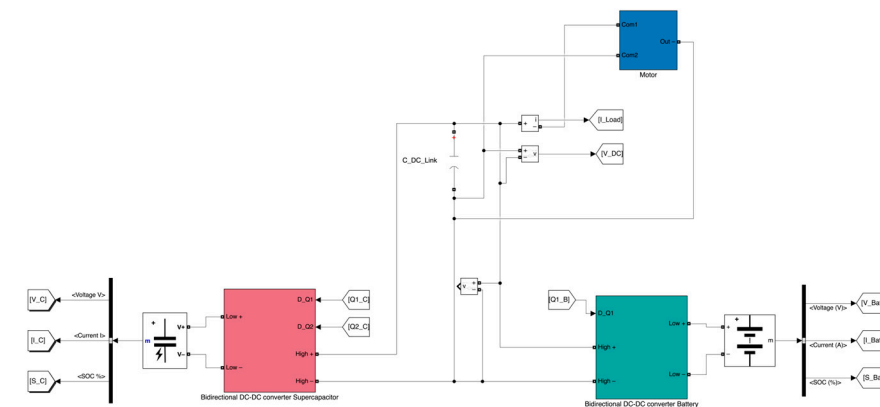

Figure 9. Fuzzy logic controller simulation using MATLAB/Simulink.

3. Results and Discussion

3.1. HESS Power Variations under Different Duty Cycles

Duty cycles play a major role in the power distribution of HESS. At low values, below 40%, the majority of power is covered by the supercapacitors due to their high-power density, so the battery pack is protected. As the duty cycles increase, batteries undertake more and more of the power demand while the ultracapacitor output becomes minimum, as depicted in Figure 10. Therefore, it is crucial to keep the duty cycle ratio as low as possible, ideally at 0.50, depending on the power state shown in Table 1.
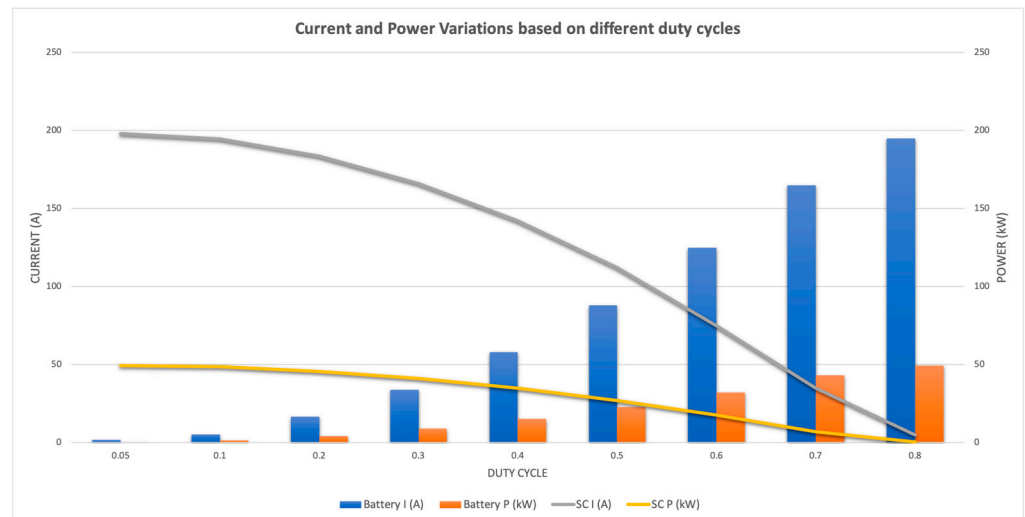

Figure 10. Power output variations of HESS based on powertrain demand and duty cycle.

3.2. Power Distribution of HESS Depending on Total Demand

The power required from the powertrain varies as the vehicle overcomes different power states; thus, the fuzzy logic controller prompts the HESS to properly distribute the power, with the rule of $SoC_{min} \geq 25\%$ without depleting any source. At the start of the simulation, after defuzzification, the motor power state is high so the ultracapacitor covers that demand while the battery supply is gradually increasing to level the power split, as represented in Figure 11. Then, after 500 ms, the motor enters a regenerative braking state so both sources are recharged quickly. Afterward, at T = 1000 ms, the acceleration state is engaged, but since the power demand is not rapid, the battery can sufficiently handle the energy needed without overheating, and the supercapacitor remains with high SoC for high-density operation occurring at T = 1250 ms. Similarly, the battery will provide power in a steady function, leading to T = 2000 ms, where the supercapacitor is reaching a lower limit based on the rules applied, so the battery has to cover the load and charge the ultracapacitor as well since demand is medium. Finally, UC is now recharged and available to cover peak loads.

Figure 12 presents the load and power distribution fluctuations shown before. Fuzzy logic controllers based on utilized rules, keep the state of charge at safe levels not leaving any source depleted, a situation that can lead to major breakdown or damage to the EV electrical systems.

The battery temperature operating range is maintained within 20–40 °C, the nominal power of the motor is 50 kW, the battery energy capacity is 40 kWh running at 360 V, and the ultracapacitor bank has a total capacitance of 5000 F at 320 V. The SoC range as stated previously, should be maintained at 20–80% effective range for both sources, but due to DC/DC converter limitations for cut-off voltage in real applications, testing mainly refers to 30% and more available SoV for the entire HESS. The dataset mainly used is available from previous work conducted [39]. However, for the previous figure, the data sequence is summarized in Table 2 below.

Figure 11. Power distribution of the hybrid storage system under different loads.
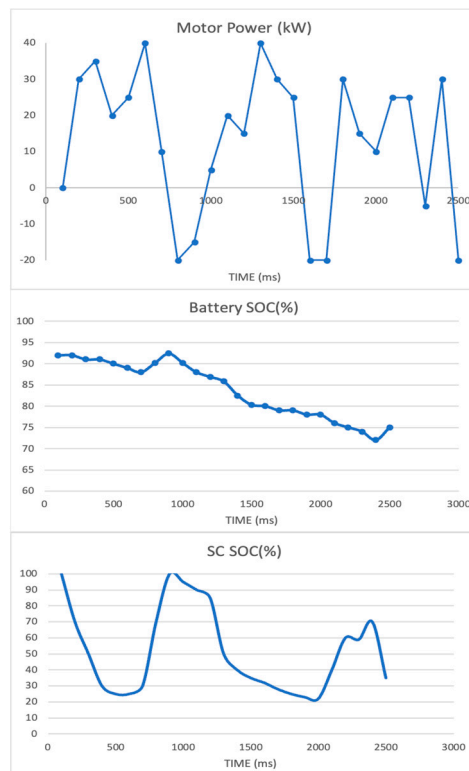

Figure 12. SOC fluctuations of the two sources separately according to the powertrain output.

Compared to a typical HESS with fuzzy rules or other management system, this work shows safe and high operation time, sufficiently prolonging battery life. With the introduction of duty cycles and constant parameter calculation, each energy source is obliged to function within a specified power, temperature, and voltage range to cover the demand of the motor or even auxiliary loads, like climate control. Based on the simulation, efficiency increases by 6% as regenerative braking utilization is highly achievable through the UC bank. The range is 2.5% boosted as HESS can cover the demand for more time, hence the distance traveled is increased. Sizing is improved by 22% as fewer batteries are required if the distance is planned as consistent and weight minimization is the requisite, while the energy source's lifetime is enhanced by 20% as battery last longer, since less stress is applied due to UC. This gain is further explained at Figure 13 below. As the charge rate increases, an energy source cannot operate for adequate amount of time. Sizing must be

sufficient, but dimensions are a key factor associated with duty cycle and useful range. Supercapacitors have an elevated ability to handle high charge rates as the left diagram explained, compared to the lithium discharge curve by [40], where the battery cells show low tolerance to high currents and charge rates, causing immense temperatures.

Table 2. Data sequence employed for Figure 12.

Time (ms)	$P_{VEHICLE}$ (kW)	SoC_{BAT} (%)	SoC_{UC} (%)
100	0	92	100
200	30	92	70
300	35	91	50
400	20	91	30
500	25	90	25
600	40	89	25
700	10	88	30
800	−20	90.2	70
900	−15	92.4	100
1000	5	90.2	95
1100	20	88	90
1200	15	86.9	85
1300	40	85.8	50
1400	30	82.5	40
1500	25	80.3	35
1600	−20	80	32
1700	−20	79	28
1800	30	79	25
1900	15	78	23
2000	10	78	22
2100	25	76	40
2200	25	75	60
2300	−5	74	59
2400	−30	72	70
2500	−20	75	35
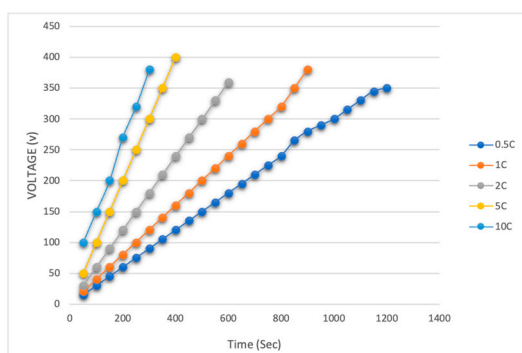
(a)
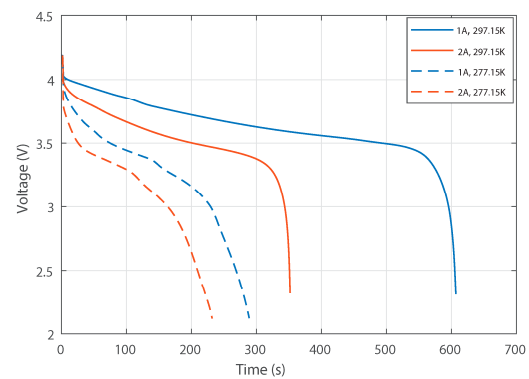
(b)

Figure 13. Difference of the two energy sources behavior and voltage output at various charge rates (**a**) Ultracapacitor operating time and voltage at five distinct rates; (**b**) Battery voltage and operating time drop at low–high charging rates and temperatures by [40].

Furthermore, the efficiency chart of the proposed method compared to the reference scheme tested in [39] is presented in Figure 14. A mean 3% efficiency improvement is available at the entire power range due to enhanced power distribution and regenerative braking utilization, except at minimal loads where the HESS is still slow in providing the supply due to DC/DC switching lag. Efficiency peaks at medium power demand, 20–30 kW, reaching 90% efficiency, including all losses from Equation (14). Motor losses are not incorporated as the HESS and converter are the main components studied in this project.
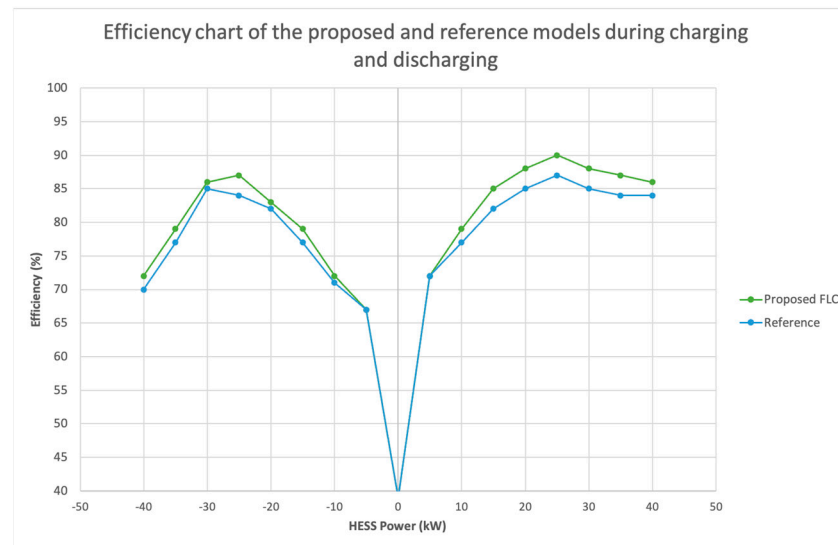

Figure 14. Efficiency chart of the experimental layout followed in [39] and this paper.

Compared to previous literature this work's novelty is the introduction of battery-safe operational zone indication, that is 20 to 80% State of charge, along with the connection of the power mode criteria with duty cycles. Depending on the power state of the engine, each source has to work in a specified duty cycle so depletion is prevented while covering the power demand completely without lag or unsafe operation. This assessment is summarized in Table 3.

Table 3. Contribution of this work supported by the latest literature.

A/A	Paper	Layout	Outcome
1	[7]	Sustainable Fuzzy Model	Power distribution through duty cycles, Utilization for lower battery stress
2	[8]	Fuzzy PID Controller	Smaller battery aging
3	[11]	Model Predictive Control	Lower battery current fluctuations, SOV indication, Single power mode
4	[13]	Fractional Order Modelling	Optimized SoC and HESS discharge time calculation
5	[19]	Semi-Active Topology	Smooth distribution for 2.5 C operation rates
6	[20]	Optimization Control for Trams	Power mode differentiation utilize better efficiency and safe operation
7	[21]	Fine tuning resistance and duty cycle method	Safe HESS Operation, battery life prolonging but higher charging time
8	[23]	Rule based Strategy with CanBUS	Power modes approach minimize Battery current and high UC employment
9	[24]	Multi-Layer Strategy on HESS	20–80% SoC indication for safe operation Single power mode

Table 3. *Cont.*

A/A	Paper	Layout	Outcome
10	[25]	Buck-Boost Converter modelling	Two power modes implementation for lower operational temperature
11	[26]	Particle Filter	Accurate state of charge calculation, with power mode introduction
12	[27]	Genetic Algorithm Optimization	Better efficiency at higher temperatures, no power modes
13	[29]	Semi-Active adaptive controller	High recovery through regenerating braking at all drive states
14	[33]	Fuzzy logic controller for electric bus	UC exploitation as primary source for better sizing, no power modes
15	[35]	Fuzzy Logic Control Optimization	Power demand-based distribution achieving 50% lower fluctuations
16	[36]	Fuzzy Logic rule-based Strategy	Duty cycle and sources SoC Consideration for better control
17	This paper	Fuzzy Logic Rule-Based Strategy	Duty cycle and power modes connection for optimized power distribution within safe Source operational range

4. Conclusions

This paper describes an energy management strategy for electric vehicles using a fuzzy logic controller for a hybrid storage system. Different power modes of the propulsion system are stated with the introduction of duty cycle importance for power distribution. Battery should be maintained within safe SoC limits (20–80%), while the ultracapacitors bank supplies the power demand as an auxiliary source and further exploits regenerative braking. The novelty of this work is the introduction and classification of power modes, providing better power distribution possibilities as duty cycles can be constantly modified, leading to better and more accurate control in real time. Power modes also indicate the driving style of the user and can be easily monitored with certain sensors, like the throttle potentiometer output. The results show that the FLC is able to regulate the power supply between the battery and the supercapacitor by changing the duty cycle value of the buck-boost converter. The proposed system is then able to adjust the power distribution according to the current power state. When the vehicle is in the acceleration state, the supercapacitor provides more or all of the power to the powertrain while the battery output gradually increases. When the vehicle is operating under normal conditions or coasting, the battery acts as the main energy source, and the ultracapacitor is utilized supportively or charging if the SoC is low. At regenerative breaking, both sources are charged depending on the converter voltage. It has been validated that duty cycles from 0.40 to 0.50 are the ideal ratios for most of the states without stressing the battery or depleting any source. This scheme achieves 6% better efficiency and 2.5% range, with 22% enhanced sizing plus 20% higher battery longevity. Future work implies testing with larger energy sources and the implementation of this management strategy in real-life applications.

Author Contributions: Conceptualization, D.R. and S.D.K.; methodology, D.R.; software, D.D.P.; validation, D.R. and S.D.K.; formal analysis, G.V.; investigation, D.R. and D.D.P.; resources, D.R.; data curation, S.D.K. and G.V.; writing—original draft preparation, D.R.; writing—review and editing, D.R. and S.D.K.; visualization, D.D.P.; supervision, S.D.K.; project administration, S.D.K. and G.V.; funding acquisition, S.D.K. All authors have read and agreed to the published version of the manuscript.

Data Availability Statement: The data that support the findings of this study are available from the corresponding author upon reasonable request.

Conflicts of Interest: The authors declare no conflict of interest.

Abbreviations

$P_{VEHICLE}$	Power demand of the Vehicle
V_H	Buck Boost converter high voltage side
I_{UC}	Ultracapacitor current
V_L	Buck-Boost converter high voltage side
I_B	Battery Current
$P_{CON,LOSS}$	Buck-Boost converter power losses
D_{BOOST}	Duty cycle on the boost mode
D_{BUCK}	Duty cycle on the buck mode
V_S	Voltage drop on the converter switch
V_D	Voltage drop on the converter diode
R_S	Resistance on the converter switch
R_L	Inductor resistance of the converter
R_D	Resistance on the converter diode
V_P	Battery polarization voltage
R_P	Battery polarization resistance
R_B	Battery internal resistance
C_P	Battery polarization capacitance
V_{OC}	Open circuit voltage
V_T	Terminal voltage
k	Time interval for the battery pack
$P_{B,LOSS}$	Battery power losses
R_{UC}	Ultracapacitor internal resistance
I_{UC}	Ultracapacitor current
C_R	Ultracapacitor rated capacitance
n	Time interval for the ultracapacitor bank
P_{UC}	Ultracapacitor power
$P_{UC,LOSS}$	Ultracapacitor power losses
V_{RATED}	Rated voltage by the manufacturer
$P_{LOSS,TOTAL}$	Total power losses
η	Powertrain efficiency
M	Vehicle mass
g	Gravitational acceleration
f	Rolling assistance coefficient
β	Road incline
C_{ARC}	Air assistance coefficient
A	Wind exposed area of the vehicle
V_A	Vehicle speed
δ	Road mass coefficient correction factor
U_R	Battery rated voltage
C_R	Battery rated voltage
n_P	Battery cells in parallel
n_S	Battery cells in series
SoC	State of Charge
SoH	State of Health

References

1. Climate Action and the Green Deal. Available online: https://commission.europa.eu/strategy-and-policy/priorities-2019-2024/european-green-deal/climate-action-and-green-deal_en (accessed on 18 August 2023).
2. Tsemekidi Tzeiranaki, S.; Economidou, M.; Bertoldi, P.; Thiel, C.; Fontaras, G.; Clementi, E.L.; Franco De Los Rios, C. The Impact of Energy Efficiency and Decarbonisation Policies on the European Road Transport Sector. *Transp. Res. Part A Policy Pract.* **2023**, *170*, 103623. [CrossRef]
3. Komnos, D.; Tsiakmakis, S.; Pavlovic, J.; Ntziachristos, L.; Fontaras, G. Analysing the Real-World Fuel and Energy Consumption of Conventional and Electric Cars in Europe. *Energy Convers. Manag.* **2022**, *270*, 116161. [CrossRef]
4. Tansini, A.; Fontaras, G.; Millo, F. A Multipurpose Simulation Approach for Hybrid Electric Vehicles to Support the European CO$_2$ Emissions Framework. *Atmosphere* **2023**, *14*, 587. [CrossRef]

5. Rimpas, D.; Kaminaris, S.D.; Aldarraji, I.; Piromalis, D.; Vokas, G.; Papageorgas, P.G.; Tsaramirsis, G. Energy Management and Storage Systems on Electric Vehicles: A Comprehensive Review. *Mater. Today Proc.* **2022**, *61*, 813–819. [CrossRef]

6. Electric Vehicles. Available online: https://www.iea.org/energy-system/transport/electric-vehicles (accessed on 18 August 2023).

7. Hartani, M.A.; Hamouda, M.; Abdelkhalek, O.; Mekhilef, S. Sustainable Energy Assessment of Multi-Type Energy Storage System in Direct-Current-Microgrids Adopting Mamdani with Sugeno Fuzzy Logic-Based Energy Management Strategy. *J. Energy Storage* **2022**, *56*, 106037. [CrossRef]

8. Zhao, Y.; Dan, D.; Zheng, S.; Wei, M.; Xie, Y. A Two-Stage Eco-Cooling Control Strategy for Electric Vehicle Thermal Management System Considering Multi-Source Information Fusion. *Energy* **2023**, *267*, 126606. [CrossRef]

9. Tran, M.-K.; Panchal, S.; Khang, T.D.; Panchal, K.; Fraser, R.; Fowler, M. Concept Review of a Cloud-Based Smart Battery Management System for Lithium-Ion Batteries: Feasibility, Logistics, and Functionality. *Batteries* **2022**, *8*, 19. [CrossRef] [PubMed]

10. Lai, X.; Yuan, M.; Tang, X.; Yao, Y.; Weng, J.; Gao, F.; Ma, W.; Zheng, Y. Co-Estimation of State-of-Charge and State-of-Health for Lithium-Ion Batteries Considering Temperature and Ageing. *Energies* **2022**, *15*, 7416. [CrossRef]

11. Chen, H.; Xiong, R.; Lin, C.; Shen, W. Model Predictive Control Based Real-Time Energy Management for a Hybrid Energy Storage System. *CSEE J. Power Energy Syst.* **2020**, *7*, 862–874. [CrossRef]

12. Liu, K.; Kang, L.; Xie, D. Online State of Health Estimation of Lithium-Ion Batteries Based on Charging Process and Long Short-Term Memory Recurrent Neural Network. *Batteries* **2023**, *9*, 94. [CrossRef]

13. Wang, Y.; Gao, G.; Li, X.; Chen, Z. A Fractional-Order Model-Based State Estimation Approach for Lithium-Ion Battery and Ultra-Capacitor Hybrid Power Source System Considering Load Trajectory. *J. Power Sources* **2020**, *449*, 227543. [CrossRef]

14. Lemian, D.; Bode, F. Battery-Supercapacitor Energy Storage Systems for Electrical Vehicles: A Review. *Energies* **2022**, *15*, 5683. [CrossRef]

15. Einan, M.; Torkaman, H.; Pourgholi, M. Optimized Fuzzy-Cuckoo Controller for Active Power Control of Battery Energy Storage System, Photovoltaic, Fuel Cell and Wind Turbine in an Isolated Micro-Grid. *Batteries* **2017**, *3*, 23. [CrossRef]

16. Zhang, Q.; Li, G. Experimental Study on a Semi-Active Battery-Supercapacitor Hybrid Energy Storage System for Electric Vehicle Application. *IEEE Trans. Power Electron.* **2020**, *35*, 1014–1021. [CrossRef]

17. Bhurse, S.S.; Bhole, A.A. A Review of Regenerative Braking in Electric Vehicles. In Proceedings of the 2018 International Conference on Computation of Power, Energy, Information and Communication (ICCPEIC), Chennai, India, 28–29 March 2018; pp. 363–367.

18. Pipicelli, M.; Sessa, B.; De Nola, F.; Gimelli, A.; Di Blasio, G. Assessment of Battery–Supercapacitor Topologies of an Electric Vehicle under Real Driving Conditions. *Vehicles* **2023**, *5*, 424–445. [CrossRef]

19. Chmielewski, A.; Piórkowski, P.; Bogdziński, K.; Możaryn, J. Application of a Bidirectional DC/DC Converter to Control the Power Distribution in the Battery–Ultracapacitor System. *Energies* **2023**, *16*, 3687. [CrossRef]

20. Lin, H.; Jiang, J.; Wei, S.; Cheng, L. Optimization Control for the Efficiency of an On-Board Hybrid Energy Storage System in Tramway Based on Fuzzy Control. In Proceedings of the 2017 11th IEEE International Conference on Compatibility, Power Electronics and Power Engineering (CPE-POWERENG), Cadiz, Spain, 4–6 April 2017; pp. 454–459.

21. Dong, A.; Ma, R.; Deng, Y. Optimization on Charging of the Direct Hybrid Lithium-Ion Battery and Supercapacitor for High Power Application through Resistance Balancing. *Energy* **2023**, *273*, 127233. [CrossRef]

22. Ghoulam, Y.; Pavot, T.; Mamouri, L.; Mesbahi, T.; Durand, S.; Lallement, C.; Kiefer, R.; Laroche, E. Energy Management Strategy with Adaptive Cut-off Frequency for Hybrid Energy Storage System in Electric Vehicles. In Proceedings of the 2022 IEEE Vehicle Power and Propulsion Conference (VPPC), Merced, CA, USA, 1–4 November 2022; pp. 1–6.

23. Xiong, R.; Duan, Y.; Cao, J.; Yu, Q. Battery and Ultracapacitor In-the-Loop Approach to Validate a Real-Time Power Management Method for an All-Climate Electric Vehicle. *Appl. Energy* **2018**, *217*, 153–165. [CrossRef]

24. Xu, W.; Liu, M.; Xu, L.; Zhang, S. Energy Management Strategy of Hydrogen Fuel Cell/Battery/Ultracapacitor Hybrid Tractor Based on Efficiency Optimization. *Appl. Sci.* **2023**, *13*, 151. [CrossRef]

25. Pai, F.S. Design and Control Method of a Battery/Ultra-Capacitor Energy Storage System for EVs. *Int. J. Electr. Electron. Eng. Telecommun.* **2023**, *12*, 203–208. [CrossRef]

26. Feng, N.; Ma, T.; Chen, C. Fuzzy Energy Management Strategy for Hybrid Electric Vehicles on Battery State-of-Charge Estimation by Particle Filter. *SN Appl. Sci.* **2022**, *4*, 256. [CrossRef]

27. Wang, C.; Liu, R.; Tang, A. Energy Management Strategy of Hybrid Energy Storage System for Electric Vehicles Based on Genetic Algorithm Optimization and Temperature Effect. *J. Energy Storage* **2022**, *51*, 104314. [CrossRef]

28. Podder, A.K.; Chakraborty, O.; Islam, S.; Manoj Kumar, N.; Alhelou, H.H. Control Strategies of Different Hybrid Energy Storage Systems for Electric Vehicles Applications. *IEEE Access* **2021**, *9*, 51865–51895. [CrossRef]

29. Hussain, S.; Ali, M.U.; Park, G.-S.; Nengroo, S.H.; Khan, M.A.; Kim, H.-J. A Real-Time Bi-Adaptive Controller-Based Energy Management System for Battery–Supercapacitor Hybrid Electric Vehicles. *Energies* **2019**, *12*, 4662. [CrossRef]

30. Yan, S.; Gu, Z.; Ding, L.; Park, J.H.; Xie, X. Weighted Memory H_∞ Stabilization of Time-Varying Delayed Takagi-Sugeno Fuzzy Systems. *IEEE Trans. Fuzzy Syst.* **2023**, 1–6. [CrossRef]

31. Zhao, X.; Zhang, Y.; Cui, X.; Wan, L.; Qiu, J.; Shang, E.; Zhang, Y.; Zhao, H. Wavelet Packet-Fuzzy Optimization Control Strategy of Hybrid Energy Storage Considering Charge–Discharge Time Sequence. *Sustainability* **2023**, *15*, 10412. [CrossRef]

32. Boumediene, S.; Nasri, A.; Hamza, T.; Hicham, C.; Kayisli, K.; Garg, H. Fuzzy Logic-Based Energy Management System (EMS) of Hybrid Power Sources: Battery/Super Capacitor for Electric Scooter Supply. *J. Eng. Res.* **2023**, S2307187723001682. [CrossRef]

33. Rocha, S.P.D.; Silva, S.M.D.; Ekel, P.I. Fuzzy Set-Based Approach for Grid Integration and Operation of Ultra-Fast Charging Electric Buses. *Int. J. Electr. Power Energy Syst.* **2022**, *138*, 107919. [CrossRef]

34. Shelma, G.; Rajeev, T. Fuzzy-Based Control Strategy for Supercapacitor Assisted Battery Powered EV. In Proceedings of the 2023 International Conference on Control, Communication and Computing (ICCC), Thiruvananthapuram, India, 19–21 May 2023; pp. 1–6.

35. Angundjaja, C.Y.; Wang, Y.; Jiang, W. Power Management for Connected EVs Using a Fuzzy Logic Controller and Artificial Neural Network. *Appl. Sci.* **2022**, *12*, 52. [CrossRef]

36. Van Jaarsveld, M.J.; Gouws, R. An Active Hybrid Energy Storage System Utilising a Fuzzy Logic Rule-Based Control Strategy. *World Electr. Veh. J.* **2020**, *11*, 34. [CrossRef]

37. Khan, M.A.; Zeb, K.; Sathishkumar, P.; Ali, M.U.; Uddin, W.; Hussain, S.; Ishfaq, M.; Khan, I.; Cho, H.-G.; Kim, H.-J. A Novel Supercapacitor/Lithium-Ion Hybrid Energy System with a Fuzzy Logic-Controlled Fast Charging and Intelligent Energy Management System. *Electronics* **2018**, *7*, 63. [CrossRef]

38. Zakzouk, N.E.; Lotfi, R.A. Power Flow Control of a Hybrid Battery/Supercapacitor Standalone PV System under Irradiance and Load Variations. In Proceedings of the 2020 10th International Conference on Power and Energy Systems (ICPES), Chengdu, China, 25–27 December 2020; pp. 469–474.

39. Rimpas, D.; Kaminaris, S.D.; Piromalis, D.; Vokas, G.; Papageorgas, P. *Design and Implementation of a Small-Scaled Hybrid Storage System for Optimal Sizing in Electric Vehicles*; AIP Publishing: Metz, France, 2023; p. 020007.

40. Sheikh, S.S.; Anjum, M.; Khan, M.A.; Hassan, S.A.; Khalid, H.A.; Gastli, A.; Ben-Brahim, L. A Battery Health Monitoring Method Using Machine Learning: A Data-Driven Approach. *Energies* **2020**, *13*, 3658. [CrossRef]